Journal of Thermal Analysis and Calorimetry (2019) 137:1255–1265
https://doi.org/10.1007/s10973-019-08054-6

The block combustion, high char residues and smoke restrain effect of nano-$FeSnO(OH)_5$ on polyvinyl chloride

He Zhao[1] · Jing Wu[1] · Wei-Dong Hu[1] · Yun-Hong Jiao[1] · Jian-Zhong Xu[1]

Received: 9 August 2018 / Accepted: 30 January 2019 / Published online: 9 February 2019

Abstract

Nanoscale and cubic-shaped $FeSnO(OH)_5$ (ITOH) flame retardant was synthesized by co-precipitation method and characterized by X-ray diffraction and transmission electron microscopy (TEM). The blank poly(vinyl chloride) (PVC0) and flexible PVC/ITOH composites were investigated by the limiting oxygen index (LOI), cone calorimetric test, tensile test and thermogravimetric analysis. The results showed that compared with PVC0, the LOI of PVC sample treated with 15 phr ITOH (PVC15) increases by 7.7%, and ITOH could more effectively promote the dehydrochlorination reaction of PVC. The flame of PVC15 disappeared for up to 165 s when it burned for 120 s, which significantly reduced the total heat release and total smoke production of PVC. This phenomenon not only can effectively prevent the proliferation of fire, but also facilitates the evacuation of people in the event of a fire. Lewis acid $FeCl_2$ and FeOCl, assigned by the Fe2p spectra of char residue, could effectively catalyze the cross-linking of PVC into carbon.

Keywords $FeSnO(OH)_5$ · Poly(vinyl chloride) · Flame retardancy · Mechanism

Introduction

Polyvinyl chloride (PVC), one of the versatile thermoplastic materials, has been widely used in various aspects, such as building materials, cable materials, pipes and frame materials [1–3]. However, high flammability is one primary problem that cannot be ignored for PVC with a large amount of flammable plasticizers, which limits the applications of PVCs [4]. In the event of a fire, PVC will generate a lot of black smoke and toxic and harmful gases, causing secondary hazards; most fire deaths are due to toxic gases, oxygen and other widely known as smoke inhalation rather than burn caused by [5]. Therefore, it is of great significance to study the flame retardant and smoke suppression of PVC.

✉ Yun-Hong Jiao
jiaoyunhonghbu@163.com

[1] Engineering Technology Research Center for Flame Retardant Materials and Processing Technology of Hebei Province, Key Laboratory of Medicinal Chemistry and Molecular Diagnosis of Ministry of Education, College of Chemistry and Environmental Science, Hebei University, No. 180 Wusi East Road, Baoding 071002, Hebei Province, China

Considerable efforts have been made to flame-retardant treatment of PVCs. Inorganic flame retardants do not produce toxic and corrosive gases and are highly safe and long lasting, environmentally friendly, low price; it is the main development direction of flame-retardant material [6]. Traditionally, inorganic flame retardants can be divided into metal hydroxides [7, 8], antimony series [9, 10], tin series [11–13], etc. Metal hydroxides, such as $Mg(OH)_2$ and $Al(OH)_3$, generally have good flame-retardant and smoke-suppressant effects as flame-retardant fillers, but a large amount of flame retardant is required to exert the flame-retardant effect [14]. The antimony series such as antimony trioxide needs to work synergistically with other substances to achieve flame-retardant and smoke-suppressant effects. Inorganic tin compounds are highly effective flame retardants and particularly suitable for flame-retardant materials containing halogen polymers [15]. In recent years, stannates have been extensively studied and applied due to their good flame-retardant and smoke-suppressant effects [16], such as $ZnSn(OH)_6$. Many documents show that iron compounds have strong smoke elimination effects [17], such as Fe_2O_3 and ferrocene ($C_{10}H_{10}Fe$). The Lewis acid and $SnCl_4$ produced during the combustion of tin also have strong flame retardancy. However, the synergistic

effects of Fe and Sn are seldom studied at home and abroad. Therefore, ITOH was synthesized and used in PVC matrix to study its flame-retardant and smoke-suppressant effect.

In this manuscript, nanoscale and cubic-shaped ITOH was synthesized successfully by co-precipitation synthesis. The flame-retardant properties of flexible PVC treated with ITOH were evaluated using limiting oxygen index (LOI), thermogravimetric analysis (TGA) and cone calorimeter (cone). The mechanical properties were also investigated. When the amount of ITOH was added to a certain value, PVC composite material will cause an interruption of combustion. The flexible PVC treated with ITOH showed the good flame-retardant and smoke-suppressant performance. At the same time, in order to study the flame-retardant mechanism of ITOH on PVC, the scanning electron microscope (SEM) and X-ray photoelectron spectroscopy (XPS) analyses were performed on the residual carbon after the cone test.

Experimental

Materials

Ferrous chloride ($FeCl_2{\cdot}4H_2O$) was purchased from Tianjin Fuchen Chemical Reagent Factory. Stannic chloride hydrated ($SnCl_4{\cdot}H_2O$) was from Tianjin Kemiou Chemical Reagent. Sodium hydroxide (NaOH) was provided by Tianjin Beichen Founder Reagent Factory. PVC resin (TL-1000, average polymerization degree = 970–1050) was obtained from Tianjin Dagulg Chemical Co. (China). Dioctyl phthalate (DOP) and heat stabilizer were from Baoding Yisida Co. (China). Coupling agent (NDZ-311) was purchased from Nanjing Shuguang of Silane Chemical Industry Co. (China). Ethyl alcohol (C_2H_6O) and lubricant were from Tianjin East China Reagent Factory. All the reagents were used as-received without further purification.

Synthesis of ITOH

The ITOH was synthesized by a co-precipitation method. First, 0.2 mol L^{-1} of $FeCl_2{\cdot}4H_2O$ and $SnCl_4{\cdot}5H_2O$ solutions and 0.8 mol L^{-1} of NaOH solution were prepared. Then, 20 mL $SnCl_4$ solution was added to 30 mL NaOH solution drop by drop, and $NaSn(OH)_6$ solution was obtained by stirring; 20 mL of $FeCl_2$ solution was added dropwise to $NaSn(OH)_6$ solution and stirred at room temperature. After 2 h, the reacted solution was centrifuged, washed three times with deionized water and absolute ethanol, respectively, and then dried in a vacuum oven at 80 °C for 12 h to obtain a sample of ITOH.

Sample preparation

Both PVC and ITOH were dried in a vacuum oven at 60 °C for 6 h before using. Samples were prepared by mixing all the raw materials and different number of flame retardants. They were blended in a two-roll mill at 150 °C for 8 min and compressed at 160 °C to form sheets, and then the sheets were cut into the test specimens. The basic formula is: PVC 100 phr, DOP 40 phr, heat stabilizer 3 phr, lubricant 1 phr, coupling agent 1 phr and a certain amount of ITOH (See Table 1 for details).

Characterization

X-ray diffraction

X-ray diffraction (XRD) patterns were obtained on a D8 Advance spectrometer, using Cu Ka (λ = 1.54056 Å) radiation. Data were collected by a step scanning procedure, with a scan speed of 0.1° s^{-1} at room temperature.

Transmission electron microscopy

The morphological information of ITOH was obtained by a Tecnai G2 F20 transmission electron microscopy (TEM). The flame-retardant sample was dispersed in ethanol and then dripped onto copper for observation.

Thermal analysis

Thermogravimetric analysis was performed on a STA 449C thermogravimetric analyzer, and set the temperature range as in 308–973 K, the heating rate were 5, 10, 15 and 20 K min^{-1}, respectively, flow rate was 60 mL min^{-1}. The ITHO was tested under air atmosphere, and PVC composites were tested under nitrogen atmosphere. Pyrolysis activation energy of PVC composites was calculated by KAS and FWO models [18–21]. KAS model: $\ln\left(\frac{\beta}{T^2}\right) = \ln\left(\frac{AE}{Rg(\alpha)}\right) - \frac{E}{RT}$. FWO model: $\ln\beta = \ln\left(\frac{AE}{Rg(\alpha)}\right) - 1.052\frac{E}{RT} - 5.33$. β is the heating rate (k min^{-1}), A is the pre-exponential factor (min^{-1}), α is the conversion rate calculated by dividing the mass loss by the total mass and $g(\alpha)$ is a function dependent on the decomposition mechanism. R is 8.314 J mol^{-1} k^{-1} as the gas constant. E is the activation energy.

Limiting oxygen index

The LOI measurement was conducted using a JF-3 oxygen index instrument according to ASTM D2863.

Table 1 Flame-retardant and tensile properties of PVC/ITOH

Sample	Loading level/phr	LOI/%	Tensile strength/MPa	Elongation/%
PVC0	0	24.9 ± 0.2	23.1 ± 0.2	297 ± 27
PVC1	1	26.5 ± 0.2	20.8 ± 0.3	225 ± 12
PVC2	2	27.7 ± 0.2	23.2 ± 1.3	289 ± 21
PVC5	5	29.1 ± 0.2	23.9 ± 0.7	247 ± 3
PVC10	10	31.7 ± 0.2	21.9 ± 1.6	234 ± 24
PVC15	15	32.6 ± 0.2	22.1 ± 0.2	230 ± 19

Tensile test

The tensile properties were tested with a UTM4204 electronic universal testing machine with a tensile rate of 200 mm min^{-1}.

Cone calorimetry

The cone test was performed on an iCone Plus cone calorimeter device according to ISO 5660 under a heat flux of 50 kW m^{-2}. The dimension of specimens was 100 mm × 100 mm × 3 mm. Parameters such as heat release rate (HRR), peak heat release rate (PHRR), total smoke production (TSP), total smoke released (TSR), total heat released (THR), remaining residue were recorded within the time of 450 s after tests started.

Scanning electron microscope

The morphology of the char residue was analyzed by a Phenom Pro X scanning electron microscope.

X-ray photoelectron spectroscopy

The X-ray photoelectron spectroscopy data were recorded by an Escalab 250Xi, using Al Kα excitation radiation with the point size of 500 μm.

Results and discussion

Characterization of ITOH

The XRD patterns of ITOH are shown in Fig. 1a. All the diffraction peaks of the cube-like precursors could be indexed to the cubic-phase ITOH (JCPDS NO.31-0654, a = 7.64 Å) [22–24]. According to the crystal plane (200) by using the Scherrer equation ($Dc = \frac{K\lambda}{\beta \cos\theta}$, where β is the full width half maximum, K = 0.94, θ is the diffraction angle and λ is the wavelength of X-rays, λ = 1.54056 Å.) [25], we can know the grain size was 45 nm. For Fig. 1b, the result of TEM shows the ITOH was nanocube particle with the size of about 70 nm.

The mass loss behavior was analyzed by using TGA-DTG, and the basic degradation information was explored. The TGA-DTG curves of ITOH under air atmosphere are shown in Fig. 2. At the thermal degradation stage, the mass loss of ITOH was about 17.70%, which was basically consistent with the theoretical dehydration level (16.30%) of ITOH. The initial decomposition temperature ($T_{5\%}$, the temperature at which the mass loss is 5%) was 470 K. The $T_{5\%}$ of ITOH was far higher than the processing temperature (433 K) of PVC.

LOI and tensile properties analysis

LOI analysis was performed to investigate the flame retardancy of pure PVC and PVC/ITOH composites, respectively, and the results are listed in Table 1. The LOI of pure PVC (PVC0) was 24.9%. When 1 phr ITOH was added, the LOI value was high to 26.5%. With incorporation of 2 phr and 5 phr ITOH, their LOI values continuously increased to 27.7% and 29.1%. While with the increase of ITOH loading level, the LOI values of PVC/ITOH composites increased to 32.6%. Table 1 also gives the tensile properties of PVC/ITOH composites. Compared with PVC0, the tensile strength of PVC2 and PVC5 increased 23.2% and 23.9%, respectively, probably resulting from the nanoparticles which had a certain reinforcing effect on the mechanical properties of PVC. Moreover, the elongation slightly decreased.

The thermal properties analysis

The mass loss behavior was analyzed by TGA for exploring the basic degradation information. The TGA curves of all the samples at 10 K min^{-1} under nitrogen atmosphere are shown in Fig. 3. The detailed data such as mass loss rate at the thermal degradation peaks and residue are listed in Table 2. As shown in Fig. 3, ITOH shows one-step mass loss. The initial decomposition temperature ($T_{5\%}$) of ITOH was 466 K, and its maximum-rate degradation temperatures (T_{m1}) and absolute value of the maximum-rate mass loss (V_{m1}) were 507 K and 2.7% min^{-1},

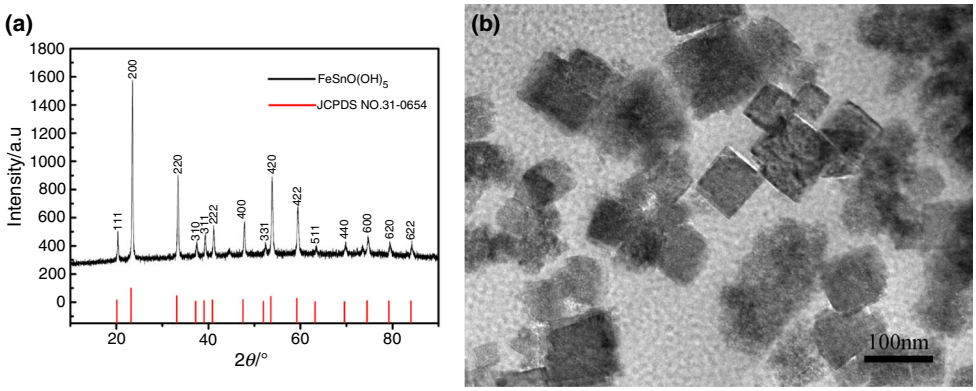

Fig. 1 XRD and TEM of ITOH

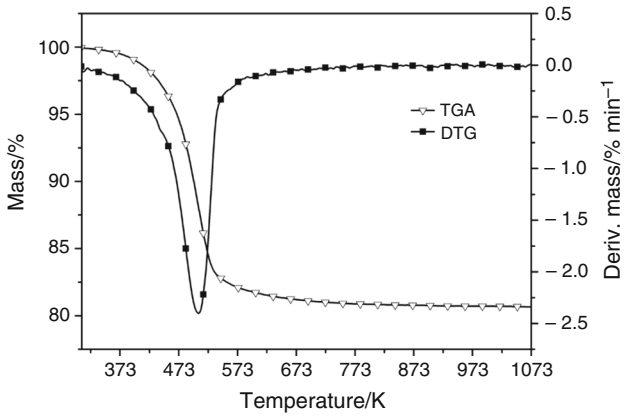

Fig. 2 TGA–DTG curves of $FeSnO(OH)_5$ tested under an air atmosphere

respectively. The main decomposition temperature range of ITOH was from 466 to 527 K.

PVC0 and PVC/ITOH composites show two-step mass loss. Compared with PVC0, the $T_{5\%}$ of PVC/ITOH composites were reduced by about 10 K. For the first stage, the mass loss of PVC0 and PVC/ITOH composites was due to the dehydrochlorination reaction of PVC and volatilization of DOP [26, 27]. From Table 2, it can be seen the T_{m1} and V_{m1} of the PVC0 were 19.1% min^{-1} and 576 K, respectively, and its decomposition temperature range (T_{R1}) was 534–617 K. The T_{R1} of PVC1, PVC2, PVC5, PVC10 and PVC15 was 73, 67, 43, 26, and 20 K, respectively, which was lower than that of the PVC0 (83 K), and with the increasing addition of ITOH, V_{m1} increased from 19.1 to 115.3% min^{-1}, which shows that the ITOH can increase the carbonization rate of PVC. For the second stage, PVC0 decomposition was due to the pyrolysis of the conjugated polyene structure, which was formed in the first stage [28]. Compared with PVC0, the decomposition temperature ranges of the second stage (T_{R2}) for PVC/ITOH composites were delayed by 26 K or so and the temperatures of maximum mass loss rate (T_{m2}) for PVC/ITOH composites were delayed by 3–14 K, which indicate that the degradation products of the PVC/ITOH composites in the first stage were more stable.

Figure 4 shows the charring efficiency of PVC/ITOH composites. The charring efficiency (E) is calculated by the following equation:

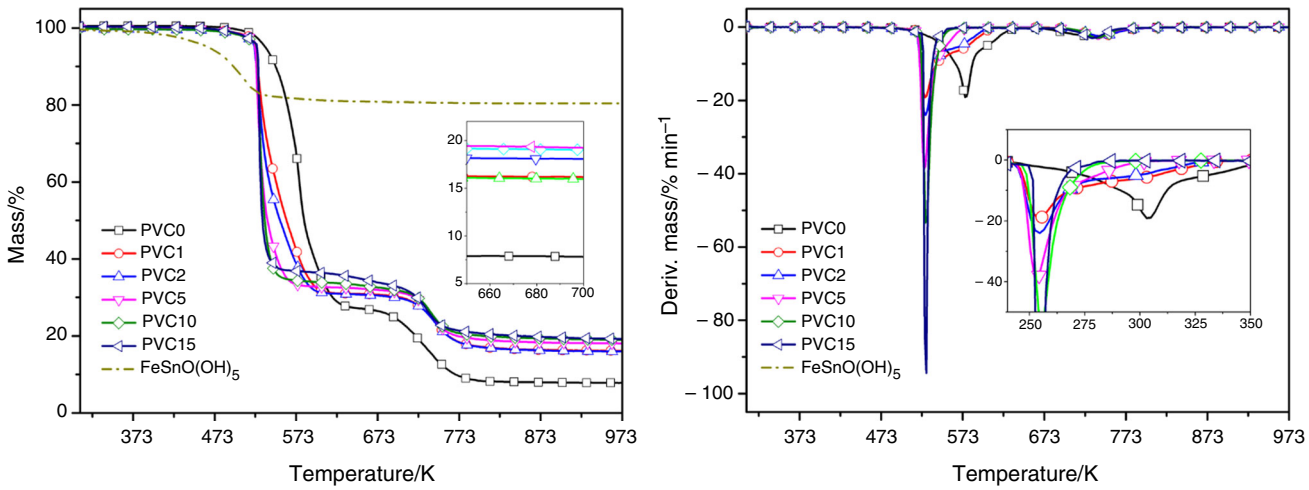

Fig. 3 TGA–DTG curves of PVC, ITOH and PVC/ITOH composites in N_2 atmosphere

Table 2 Thermogravimetric data of the PVC, ITOH and PVC/ITOH composites in N_2 atmosphere

Sample	$T_{-5\%}$/K	T_{R1}/K	T_{m1}/K	V_{m1}/% min^{-1}	T_{R2}/K	T_{m2}/K	V_{m2}/% min^{-1}	Residue/%
PVC0	534	534–650	576	19.1	688–769	930	2.5	7.8
PVC1	523	523–596	527	19.2	684–769	742	2.5	16.1
PVC2	522	522–589	527	24.0	717–769	744	2.6	16.0
PVC5	522	522–565	526	39.6	717–762	733	3.2	18.1
PVC10	525	525–551	528	55.3	717–760	736	3.0	19.0
PVC15	526	526–546	527	115.3	708–753	733	3.3	19.3
$FeSnO(OH)_5$	466	466–527	507	2.7	–	–	–	80.4

$$A(1+x)a + B(1+E)b = c \quad (1)$$

where A and B are the mass percentage of flame retardant and PVC, respectively; a, b and c are the residue of flame retardant, PVC and PVC/ITOH composites, respectively; and x (< 0) is the percentage of flame retardant reacted after flame-retardant PVC. When the flame retardant reacted completely and did not remain in the residue, the char formation efficiency of the flame retardant was as shown in Fig. 4. The results show that E increased with the increase in the number of flame-retardant additions. E was the highest when 15 phr ITOH was added.

Kinetic analysis

In order to further prove that ITOH can produce effective flame-retardant effect in PVC aggregates, the non-isothermal decomposition kinetics method was used to further study the PVC0 and PVC15.

Figure 5 shows the TGA and DTG curves of PVC0 and PVC15 pyrolysis at heating rates of 5, 10, 15 and 20 K min^{-1} at nitrogen atmosphere. Because the material has two-step decomposition, the calculation of pyrolysis kinetics will be divided into two parts. Two different algorithms KAS and FWO models were used to calculate the activation energy of materials. Figure 6 is a linear fit plot for determining activation energy of the PVC0 and PVC15 in the first stage. Conversion rate was 0.1, 0.2, 0.3, 0.4, 0.5 and 0.6, respectively. The activation energy data are shown in Table 3. The average activation energies of the first-stage decomposition of PVC0 calculated by KAS and FWO models were 121.62 and 124.67 kJ mol^{-1}, respectively. The deviation was 2.4%. The average activation energies of the first-stage decomposition of PVC15 were 129.91 and 132.12 kJ mol^{-1}, respectively. The deviation was 1.7%. It shows that the activation potential calculated by KAS and FWO models is credible. The average activation energy of PVC15 calculated by KAS and FWO models was larger than that of PVC0, which indicates that the prepared ITOH can play a flame-retardant role in the application of PVC. At the same time, the activation energy of the second stage of pyrolysis was calculated by the same method. Figure 7 is a linear fit plot for determining activation energy of the PVC0 and PVC15 in the second stage. While the conversion of PVC0 was 0.78, 0.80, 0.82, 0.84, 0.86, the conversion of PVC15 was 0.68, 0.70, 0.72, 0.74 and 0.76, respectively. The activation energy data are shown in Table 4. The average activation energies of the second-stage decomposition of PVC0 calculated by KAS and FWO models were 191.45 and 204.09 kJ mol^{-1}, respectively. The average activation energies of the second-stage decomposition of PVC15 were 191.74 and 204.28 kJ mol^{-1}, respectively. By comparing the data in Table 4, we can see that the activation energies produced by the decomposition of PVC0 and PVC15 in the second stage are basically similar. Combining with Table 3, it shows that ITOH decomposes mainly in the first stage and has obvious flame-retardant effect, but not in the second stage.

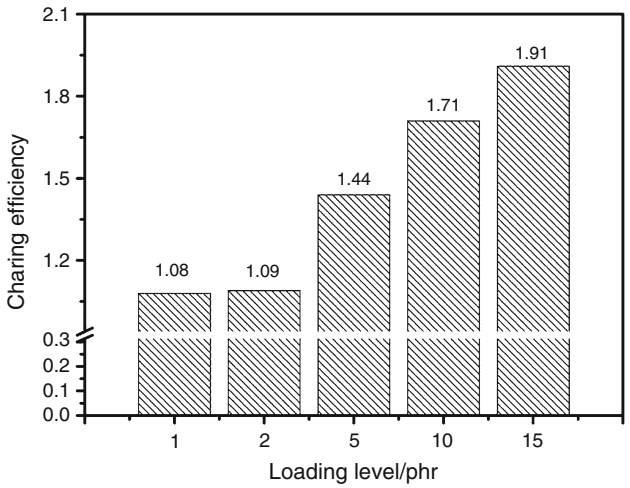

Fig. 4 Charring efficiency of PVC/ITOH composites

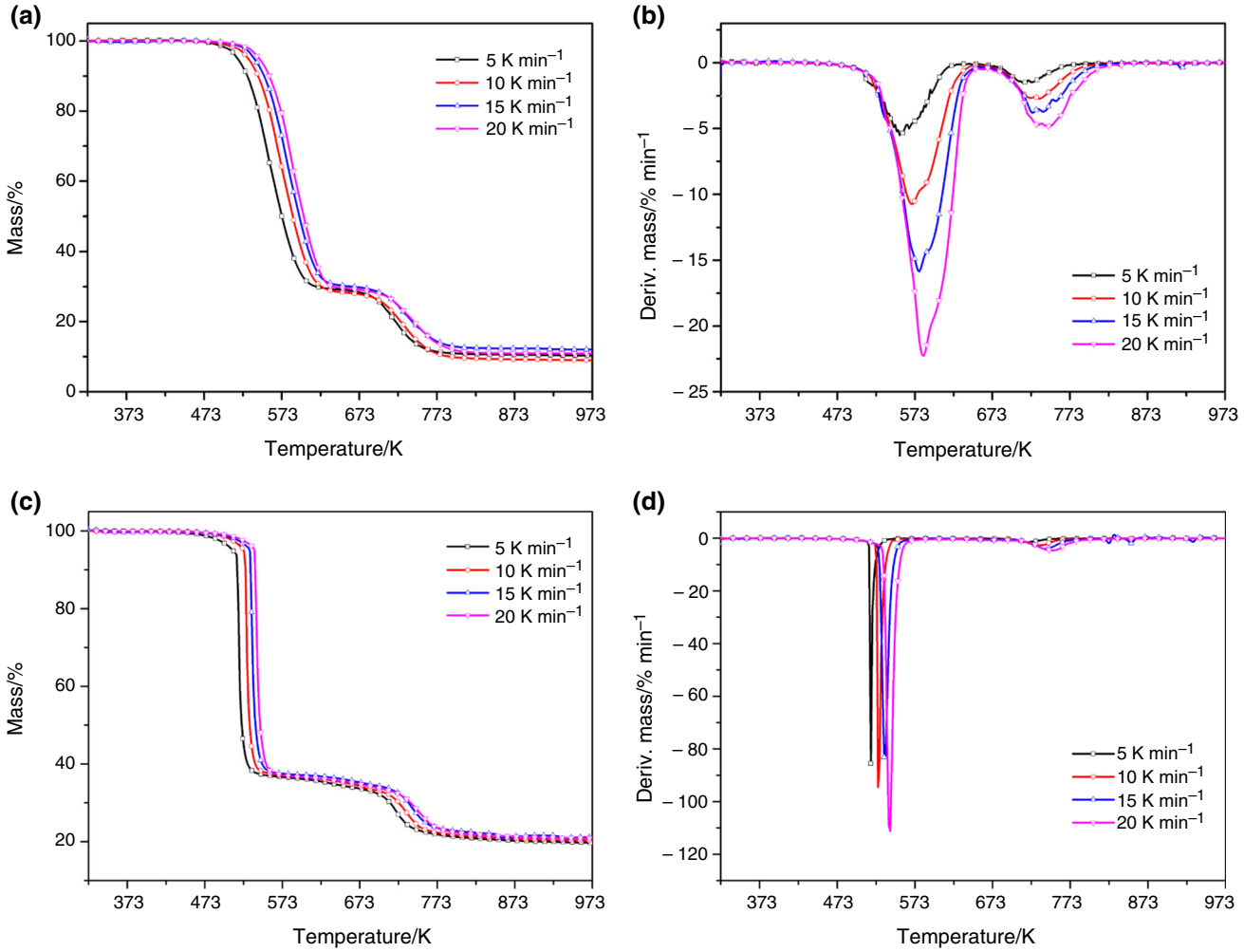

Fig. 5 TGA and DTG curves of PVC0 and PVC15 pyrolysis at heating rates of 5, 10, 15 and 20 K min^{-1} at under nitrogen atmosphere: **a** TGA curve of PVC0, **b** DTG curve of pvc0, **c** TGA curve of pvc15, **d** DTG curve of pvc15

The combustion behaviors analysis

The combustion behavior of PVC0 and PVC/ITOH composites had been investigated by cone calorimeter. The curves of heat release rate (HRR), and smoke production rate (SPR) are presented in Fig. 8. And the acquired data are depicted in Table 5, such as total heat release (THR), the peak of HRR (PHRR), total smoke rate (TSR) and the peak of SPR (PSPR).

In Fig. 8a, the HRR curve of PVC0 had a peak with the peak heat release rate (PHRR) value of 330 kW m^{-2} and the HRR curves of PVC5 and PVC15 were attenuated into two small peaks, where the higher peaks of PVC5 and PVC15 were reduced by 31.2% and 53.6%, respectively, compared to PVC0. At 110 s, the HRR curve of PVC15 plummets, resulting in a very low HRR of approximately 17–32 kW m^{-2} at 130-295 s, due to the disappearance of flame within 130–295 s during the cone test. This phenomenon not only can effectively prevent the spread of fire, but also facilitates the evacuation of people in the event of a fire. And the THR of PVC5 and PVC15 was lower than that of PVC0 and reduced by 20.0% and 48.1%, respectively (Table 5). From Fig. 8b, it can be seen that the peak SPR (PSPR) of PVC5 and PVC15 was lower than PVC0 and reduced by 54.1% and 81.1% respectively. And the TSR of PVC5 and PVC15 was reduced by 57.4% and 66.1%, respectively (Table 5). These results show that ITOH has a good flame-retardant and smoke-suppressant effect on PVC.

Fire performance index (FPI) indicates the magnitude of fire risk [29], the ratio of the ignition time (TTI) to the phrR, which are summarized in Table 5. The FPI of PVC0 was 0.039 s m^2 kW^{-1} (FPI < 1), and that of PVC5 and PVC15 increased to 0.066 s m^2 kW^{-1} and 0.092 s m^2 kW^{-1}. This shows that the PVC/ITOH composites have less fire hazard and ITOH has better flame-retardant performance. The residue of PVC0 was 3.5%, and that of PVC5 and PVC15 was increased by 257% and 349%, respectively, compared

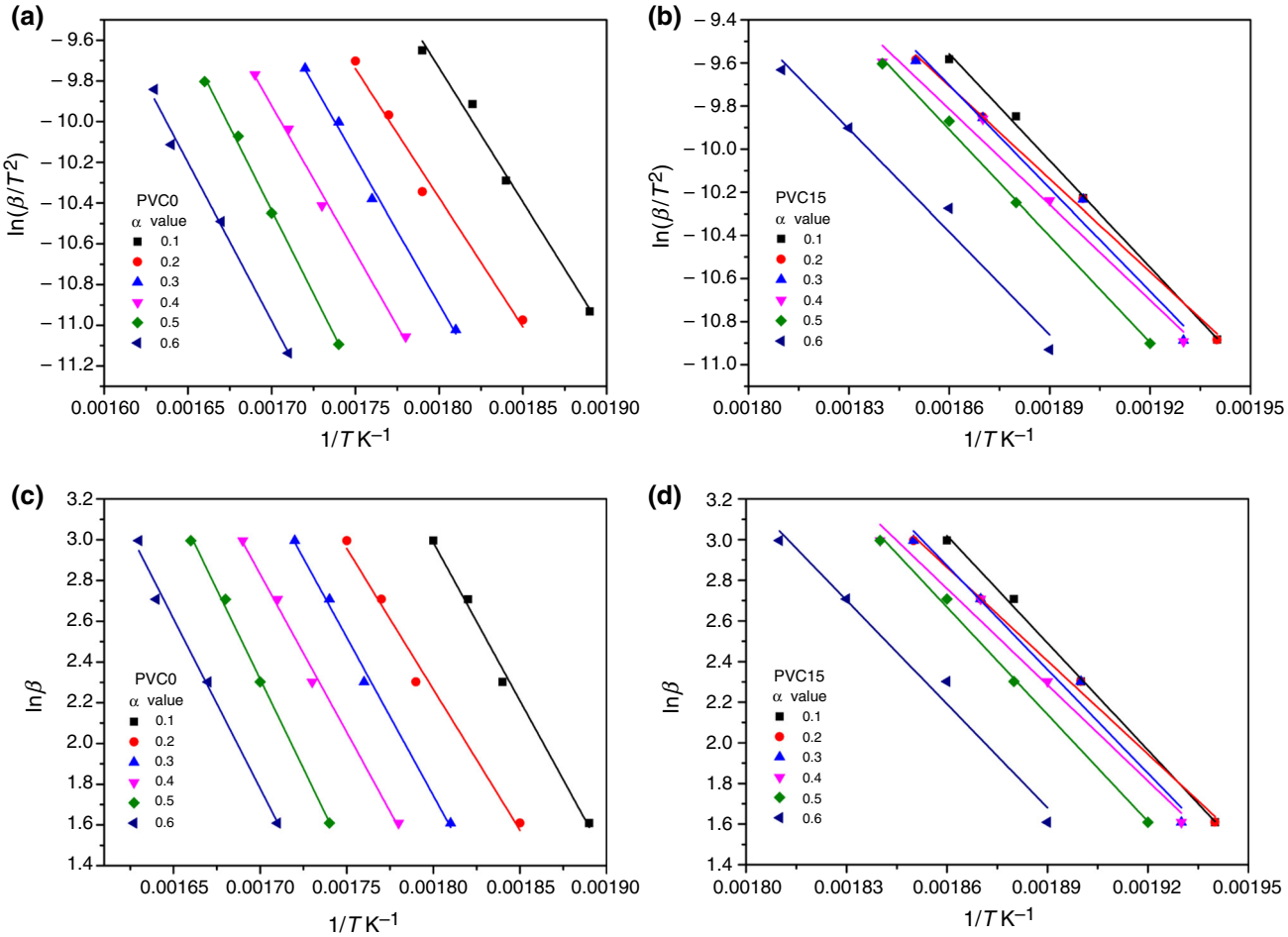

Fig. 6 Linear fit plot for determining activation energy of the PVC0 and PVC15 in the first stage. **a** KAS curve of PVC0, **b** KAS curve of PVC15, **c** FWO curve of PVC0, **d** FWO curve of PVC15

Table 3 Activation energies/*E* for different conversion values obtained by KAS and FWO models in the first stage

Conversion/α	KAS model *E*/KJ mol^{-1}		FWO model *E*/KJ mol^{-1}	
	PVC0	PVC15	PVC0	PVC15
0.1	111.41	132.44	122.70	138.94
0.2	101.86	131.69	109.27	121.11
0.3	119.34	129.19	122.70	134.51
0.4	125.39	128.11	122.70	124.69
0.5	131.21	128.99	138.94	138.94
0.6	140.50	129.04	131.70	134.51
Average	121.62	129.91	124.67	132.12

with PVC0. The increase of residues is attributed to char formation due to the excellent catalytic performance of ITOH, which is agreement with the behavior of heat release. TTI values of the PVC5 and PVC15 are a little higher than the PVC0, which also suggested that the addition of ITOH improves the flam retardancy of PVC.

Char residue analysis

In order to study the flame-retardant mechanism of ITOH, the char residue after the cone test was further analyzed. Figure 9 shows the digital photograph of char residue. PVC0 had almost no residual char residue, indicating that pure PVC is almost completely decomposed. The surface of PVC5 sample residue was loose, and the pores were relatively large. Moreover, the char of PVC5 was red, which indicated that there were iron compounds in this char. The residual char of PVC15 was relatively compact with a light red color. The results show that ITOH is favorable for the catalysis of PVC charring.

Figure 10 shows the SEM photographs of the inner char residue for PVC0 and PVC composites. There were many holes in the char layer on the inner surface of the PVC0 from Fig. 10a. Compared with PVC0, the char residues of

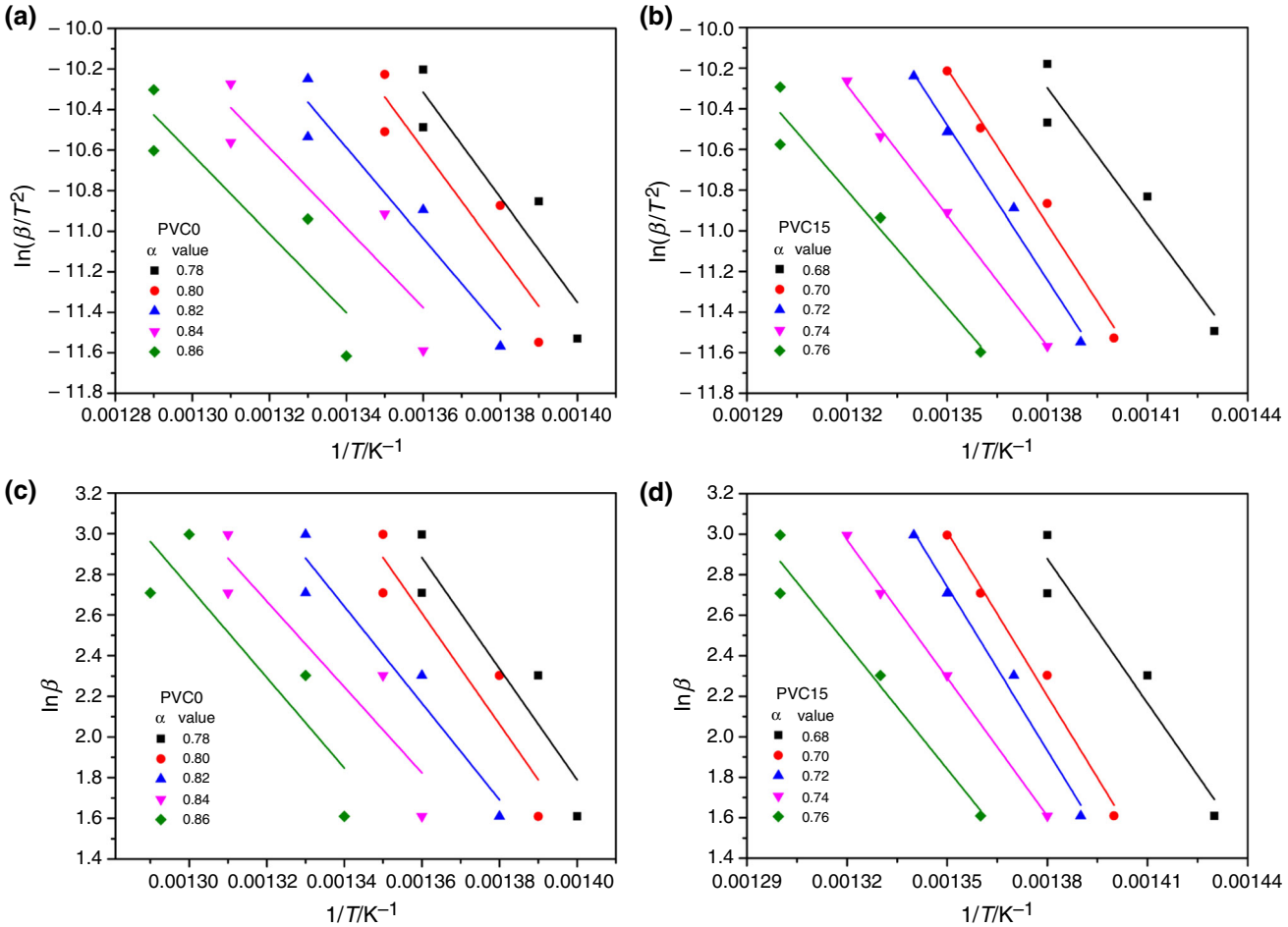

Fig. 7 Linear fit plot for determining activation energy of the PVC0 and PVC15 in the second stage. **a** KAS curve of PVC0, **b** KAS curve of PVC15, **c** FWO curve of PVC0, **d** FWO curve of PVC15

Table 4 Activation energies/*E* for different conversion values obtained by KAS and FWO models in the second stage

Conversion/α	KAS model *E*/KJ mol^{-1}		Conversion/α	FWO model *E*/KJ mol^{-1}	
	PVC0	PVC0		PVC15	PVC15
0.78	221.07	233.12	0.68	193.68	207.24
0.80	211.32	223.49	0.70	201.03	213.10
0.82	196.40	208.70	0.72	196.24	208.44
0.84	179.90	192.34	0.74	192.02	204.35
0.86	148.58	162.81	0.76	175.74	188.27
Average	191.45	204.09	Average	191.74	204.28

PVC5 and PVC15 were denser. There were more vesicle structures on the char layer of PVC5 (Fig. 10b), probably because PVC5's char layer is thinner and looser than PVC15's. And in Fig. 10c, there were a lot of folds on the char layer of PVC15, which indicate that the residual char has good toughness and flame-retardant effect.

XPS can analyze the composition and elements content of the char residue, so the char residue of PVC15 is analyzed as shown in Figs. 11 and 12. Figures 11 and 12 present that in addition to containing more C and O elements, there were Cl, Fe and trace of Sn in the char residue. The results show that the effect of iron on the inhibition of halogenation of the halogen-containing polymer mainly occurred in the solidification phase; tin was reduced by the reducing gas to $SnCl_2$ (boiling point of 623 °C.) in the combustion process and most of the volatilization to the gas phase [30, 31].

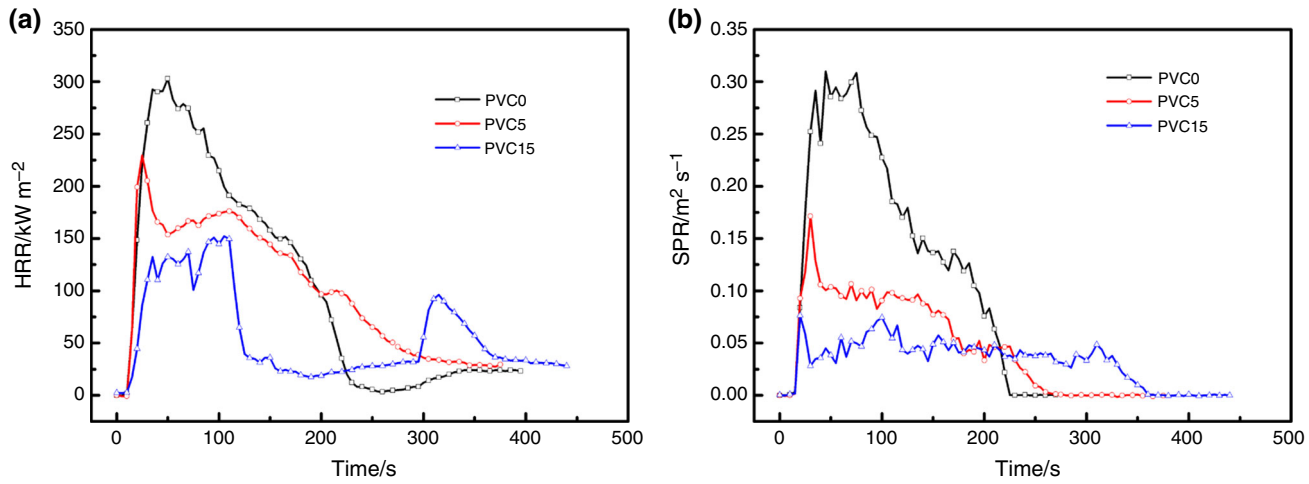

Fig. 8 HRR and SPR curves of PVC0 and PVC/ITOH composites: **a** HRR curves and **b** SPR curves

Table 5 Data obtained from cone test

Sample	PHRR/kW m^{-2}	tPHRR/s	THR/MJ m^{-2}	PSPR/m^2 s^{-1}	TSR/m^2 m^{-2}	TTI/s	FPI/s m^2 kW^{-1}	Residue/%
PVC0	330	55	47.6	0.37	4772	13	0.039	3.5
PVC5	227/176	25/110	38.1	0.17	2035	15	0.066	12.5
PVC15	153/96	135/315	24.7	0.07	1619	14	0.092	15.7

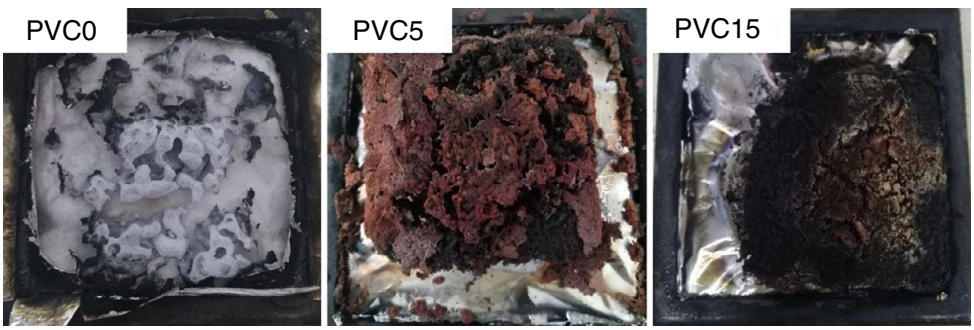

Fig. 9 Digital photographs of char residues

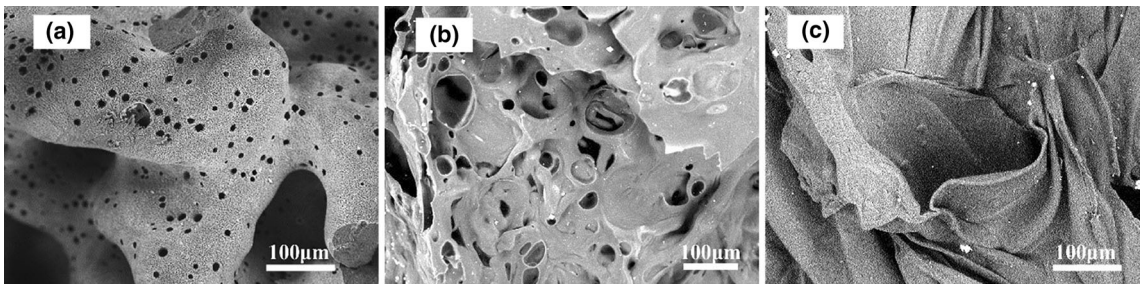

Fig. 10 SEM of char residues: **a** PVC0, **b** PVC5 and **c** PVC15

In order to understand the presence of Fe in the char residue, the XPS curve of Fe2p was fitted, which is shown in Fig. 13. The energy calibration was made with the C 1*s* (E_b = 284.6 eV) level of adventitious carbon. There were two combinations of Fe2p in the residue of PVC15, including FeOCl (726.0 eV, Fe2$p_{1/2}$ and 712.9 eV, Fe2$p_{3/2}$) and $FeCl_2$ (723.7 eV, Fe2$p_{1/2}$ and 710.6 eV, Fe2$p_{3/2}$). The result shows that the ITOH flame retardant produced FeOCl

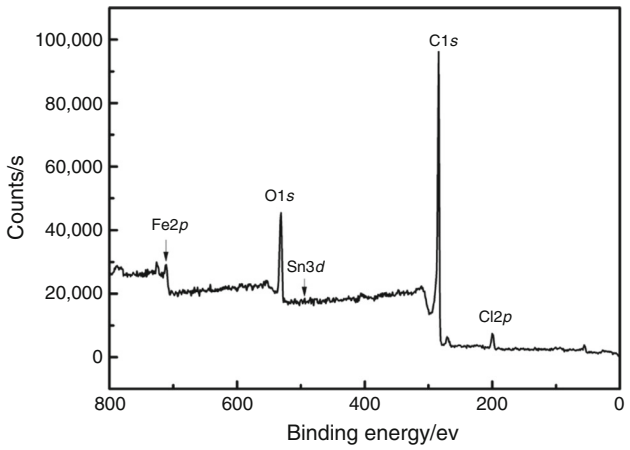

Fig. 11 XPS spectra of char residue of the PVC15

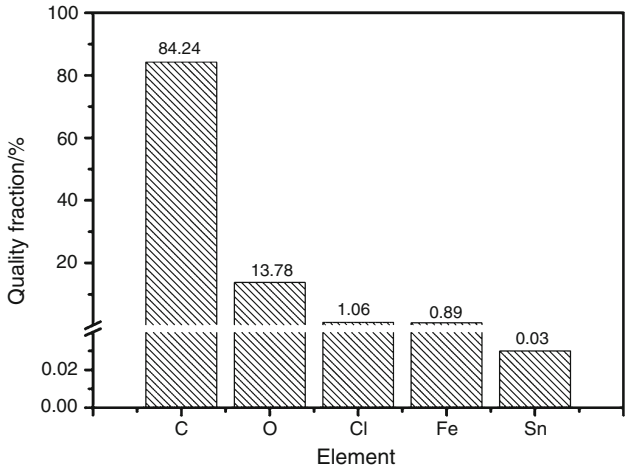

Fig. 12 Element content of char residue of the PVC15

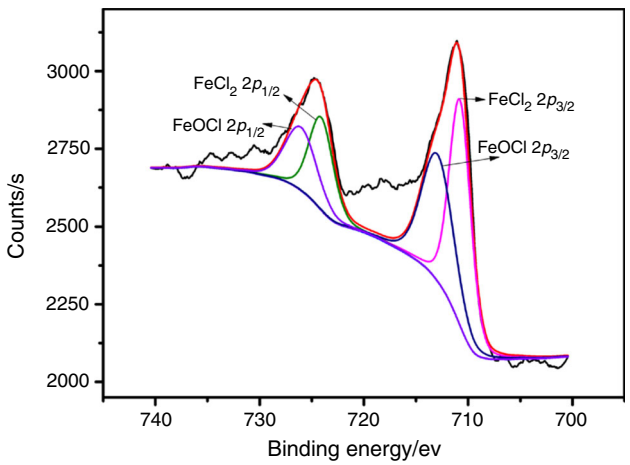

Fig. 13 Curve-fitting results of the Fe2*p* spectra of char residue of the PVC15

in situ, and FeOCl could produce a Lewis acid cross-linking reaction and catalyze the formation of a large amount of carbon residue; a part of the ITOH undergoes a complex oxidation–reduction reaction to generate $FeCl_2$. Its Lewis acidity is weak, and it can also catalyze certain Friedel–Crafts cross-links that are conducive to flame retardance and smoke suppression, but do not promote the pyrolysis of the carbon layer.

Conclusions

Nanoscale and cubic-shaped ITOH flame retardant was synthesized by co-precipitation method. ITOH can effectively increase the LOI of PVC, had less impact on the mechanical properties of PVC. TGA, DTG and kinetic analysis results showed that ITOH can more effectively promote the dehydrochlorination reaction of PVC and the degradation products of the PVC/ITOH composites were more stable in the first stage. Cone results showed ITOH can effectively reduce the heat release and smoke emission of PVC. When ITOH was added to 15 phr, the flame of PVC15 disappeared for up to 165 s when it burned for 120 s. This phenomenon not only can effectively prevent the spread of fire, but also facilitates the evacuation of people in the event of a fire. The results of char residue show that the residual carbon of the ITOH-added PVC sample is tighter and denser, and the flame-retardant effect of ITOH on PVC is mainly to produce Lewis acid $FeCl_2$ and FeOCl, which can effectively catalyze the cross-linking of PVC into carbon.

References

1. Jia P, Zhang M, Hu L, Feng G, Zhou Y. Synthesis of novel caged phosphate esters and their flame retardant effect on poly(vinyl chloride) blends. Chem Lett. 2015;44(9):1220–2.
2. Carroll WF, Johnson RW, Moore SS, Paradis RA (2017) 4–Poly(vinyl chloride). In: Kutz M, editor. Applied plastics engineering handbook, 2nd ed. The Vinyl Institute, Alexandria, VA: Matthew Deans; 2017. p. 73–89.
3. Sun YJ, Gao M, Chai ZH, Wang H. Thermal behavior of the flexible polyvinyl chloride including montmorillonite modified with iron oxide as flame retardant. J Therm Anal Calorim. 2018;131:65–70.
4. Ou YX, Chen Y, Wang XM. Flame-retarded polymeric materials. Beijing: National Defense Industry Press; 2001. p. 16–9.
5. Liu X, Wang JY, Yang XM, Wang YL, Hao JW. Application of TG/FTIR TG/MS and cone calorimetry to understand flame retardancy and catalytic charring mechanism of boron phosphate in flame-retardant PUR-PIR foams. J Therm Anal Calorim. 2017;130:1817–27.
6. Jiao YH, Wang X, Peng F, Xu JZ, Gao JG, Meng HJ. Increased flame retardant, smoke suppressant and mechanical properties of semi-rigid polyvinyl chloride (PVC) treated with zinc hydroxystannate coated dendritic fibrillar calcium carbonate. J Macromol Sci B. 2014;53(3):541–54.

7. Klapiszewski L, Tomaszewska J, Skórczewska K, Jesionowski T. Preparation and characterization of eco-friendly $Mg(OH)_2$ lignin hybrid material and its use as a functional filler for poly(vinyl chloride). Polymers. 2017;9(7):258.
8. Zhang ZF, Wu WH, Zhang MJ, Qu JM, Shi L, Qu HQ, et al. Hydrothermal synthesis of 4ZnO center dot B_2O_3 center dot H_2O/RGO hybrid material and its flame retardant behavior in flexible PVC and magnesium hydroxide composites. Appl Surf Sci. 2017;425:896–904.
9. Basfar AA. Flame retardancy of radiation cross-linked poly(vinyl chloride) (PVC) used as an insulating material for wire and cable. Polym Degrad Stab. 2002;77(2):221–6.
10. Schartel B, Kunze R, Neubert D, Tidjani A. ZnS as fire retardant in plasticised PVC. Polym Int. 2002;51(3):213–22.
11. Sang B, Li Z, Yu L, Li X, Zhang Z. Preparation of zinc hydroxystannate-titanate nanotube flame retardant and evaluation its smoke suppression efficiency for flexible polyvinyl chloride matrix. Mater Lett. 2017;204:133–7.
12. Zhang B, Han J. Morphology control of zinc hydroxystannate microcapsules by sol-gel method and their enhanced flame retardancy properties for polyvinyl chloride composites. J Sol–Gel Sci Technol. 2017;81(2):442–51.
13. Zhang B, Liu H, Han J. Zinc hydroxystannate microencapsulated to improve its safety and application to flame-retardant, smoke-suppressed polyvinyl chloride composites. J Alloys Compd. 2017;712:768–80.
14. Yang G, Wu WH, Dong HX, Wang YH, Qu HQ, Xu JZ. Synergistic flame-retardant effects of aluminum phosphate and trimer in ethylene–vinyl acetate composites. J Therm Anal Calorim. 2018;132:919–26.
15. Kicko-Walczak E. Study on flame retardant unsaturated polyester resins-an overview of past and new developments. Polimery. 1999;44(11–12):724–9.
16. Xu JZ, Zhang CY, Qu HQ, et al. Zinc hydroxys-tannate and zinc stannate as flame retardant agents for flexible PVC. J Appl Polym Sci. 2005;98:1469–75.
17. Sun YJ, Gao M, Chai ZH, Wang H. Thermal behavior of the flexible polyvinyl chloride including montmorillonite modified with iron oxide as flame retardant. J Therm Anal Calorim. 2017;131:65–70.
18. Kissinger HE. Reaction kinetics in differential thermal analysis. Anal Chem. 1957;29:1702–6.
19. Akahira T, Sunose T. Method of determining activation deterioration constant of electrical insulating materials. Res Rep Chiba Inst Technol (Sci Technol). 1971;16:22–31.
20. Ozawa T. A new method of analyzing thermogravimetric data. Bull Chem Soc Jpn. 1965;38:1881–6.
21. Flynn JH, Wall LA. A quick, direct method for the determination of activation energy from thermogravimetric data. J Polym Sci B Polym Phys. 1966;4:323–8.
22. Nakayama N, Kosuge K, Kachi S, Shinjo T, Takada T. Magnetic properties of $FeSn(OH)_6$ and its oxidation product $FeSnO(OH)_5$. Mater Res Bull. 1978;13(1):17–22.
23. Welch MD, Kampf AR. Stoichiometric partially-protonated states in hydroxide perovskites: the jeanbandyite enigma revisited. Miner Mag. 2017;81(2):297–303.
24. Huanga D, Fuac X, Longc J, Jianga X, Changa L, Menga S, et al. Hydrothermal synthesis of $MSn(OH)_6$ (M = Co, Cu, Fe, Mg, Mn, Zn) and their photocatalytic activity for the destruction of gaseous benzene. Chem Eng J. 2015;269:168–79.
25. Selvi J, Mahalakshmi S, Parthasarathy V. Synthesis, structural, optical, electrical and thermal studies of poly(vinyl alcohol)/CdO nanocomposite films. J Inorg Organomet Polym Mater. 2017;27(6):1918–26.
26. Qi YX, Wu WH, Han LJ, Qu HQ, Han X, Wang AQ, et al. Using TG-FTIR and XPS to understand thermal degradation and flame-retardant mechanism of flexible poly(vinyl chloride) filled with metallic ferrites. J Therm Anal Calorim. 2015;123(2):1263–71.
27. Xu JZ, Jiao YH, Zhang B, Qu HQ, Yang GZ. Tin dioxide coated calcium carbonate as flame retardant for semirigid poly(vinyl chloride). J Appl Polym Sci. 2006;101(1):731–8.
28. Qu HQ, Wu WH, Wei HY, Xu JZ. Metal hydroxystannates as flame retardants and smoke suppressants for semirigid poly(vinyl chloride). J Vinyl Addit Technol. 2008;14(2):84–90.
29. Subasinghe A, Das R, Bhattacharyya D. Parametric analysis of flammability performance of polypropylene/kenaf composites. J Mater Sci. 2016;51(4):2101–11.
30. Herzler J, Roth P. Shock tube study of the reaction of H atoms with $SnCl_4$. ChemInform. 2002;21:5259–64.
31. Li ZW, Shao B, Huang YS, Li XH, Zhang ZJ. Effect of core-shell zinc hydroxystannate nanoparticle-organic macromolecule composite flame retardant prepared by masterbatch method on flame-retardant behavior and mechanical properties of flexible poly(-vinyl chloride). Polym Eng Sci. 2014;54(9):1983–9.